Direct Experiments on the Ocean Disposal of Fossil Fuel CO_2

Peter G. Brewer,[1]* Gernot Friederich,[1] Edward T. Peltzer,[1] Franklin M. Orr Jr.[2]

Field experiments were conducted to test ideas for fossil fuel carbon dioxide ocean disposal as a solid hydrate at depths ranging from 349 to 3627 meters and from 8° to 1.6°C. Hydrate formed instantly from the gas phase at 349 meters but then decomposed rapidly in ambient seawater. At 3627 meters, the seawater–carbon dioxide interface rose rapidly because of massive hydrate formation, forcing spillover of the liquid carbon dioxide from the container. A strong barrier between the liquid carbon dioxide and interaction with the sediments was observed. A pool of liquid carbon dioxide on the sea floor would expand in volume more than four times, forming hydrate, which will dissolve.

One possibility for the disposal of fossil fuel CO_2, in order to forego atmospheric emissions and the concomitant enhancement of the atmospheric greenhouse effect, is to place it in the deep ocean (*1*). Fossil fuel CO_2 in the atmosphere is already passively absorbed by the ocean, in the amount of some 2 GT of carbon per year (*2*). The invading wave of atmospheric CO_2 has already dramatically altered the chemistry of surface seawater worldwide (*3*), and over much of the ocean this tracer field has now penetrated to a depth of >1 km.

We conducted a set of deep-sea experiments on the direct injection of CO_2 in both the liquid and gas phase into seawater under various pressure and temperature conditions (*4, 5*). The experiments were carried out to extend laboratory pressure vessel studies (*6*) to real world conditions and to begin evaluating the various models proposed for disposal of fossil fuel CO_2 in seawater. The advantages of ocean experiments lie in their fidelity as tests for industrial processes, their incorporation of the fluid dynamics and reactions of the open release, and the ability to study marine biological responses and sediment geochemical interactions.

Two key features make deep ocean disposal attractive. First, because of the large size of the ocean and the geochemical buffer provided by the alkalinity of seawater, $[(\Delta P_{CO_2}/P_{CO_2})/(\Delta T_{CO_2}/T_{CO_2})] \approx 10$ (P = pressure and T = temperature), and the carbonate sediments, little disposed material will return to the atmosphere (*7*). Second, CO_2 can react with water at low temperature and high pressure to form a solid hydrate (*8*), which might sequester CO_2 from the geochemical cycle. Much uncertainty surrounds the process. Although pure CO_2 hydrate is denser than seawater and will sink, in practice occluded gas and liquid can make globules rise (*6*). Formation of hydrate is exothermic, and the release of heat and rejection of salt may generate local instabilities that strongly affect the system.

We carried out a series of five experiments off the coast of central California. At an appropriate temperature and pressure (Fig. 1), CO_2 in excess of that required to saturate the surrounding seawater may exist as a gas and will react to form a hydrate. In an experiment conducted at a depth of 349 m and at 8°C, we released CO_2 into an inverted glass beaker. A mass of bright, white hydrate with occluded gas formed immediately along with a bubble of excess gas at the top of the beaker (Fig. 2). Compression of the mass of hydrate and gas bubbles as the vehicle descended below 349 m caused flakes of hydrate to fall into the ambient seawater outside the beaker, where they appeared to dissolve in seconds (*9*).

We released about 50 ml of liquid CO_2 (*10*) at a depth of 430 m into an inverted beaker. The liquid mass became coated with a thin hydrate film, but the ensemble was strongly buoyant because of density differences between liquid CO_2 and seawater. When the CO_2 mass was released, it broke down into smaller globules that rose rapidly. It was possible to fly the 3000-kg vehicle upward at a rate equal to the rise rate of the released CO_2 (18 to 20 m/min) and to maintain visual contact with the plume as it passed through the liquid-gas phase boundary. Estimation of the ascent rate of a CO_2 release within the hydrate-forming region has been the object of much study (*6*) and is an essential goal of large CO_2 release experiments being planned (*11*). Visual contact was lost shortly after the gas-phase boundary was crossed.

The method of injection caused changes in the surface area of the hydrate formed and in its dissolution rate. At a depth of 905 m we created, by vigorously injecting liquid CO_2 through a narrow-bore tube, a mass of flocculant hydrate (Fig. 3), completely filling the inverted 2-liter beaker. The hydrate remained trapped and buoyant. The apparatus was left moored in place; 17 days later, all the hydrate had disappeared either by dissolution in the beaker or by sinking into the surrounding water. The result of a much slower release of liquid CO_2 at this depth into a 1-liter reaction chamber was that a two-layer CO_2-water system, stable for the several hours of observation, was formed. Even mechanical mixing back and forth across the interface did not create a hydrate mass; thus, energetic water-CO_2 mixing is required to promote large-scale hydrate formation.

At 2°C and at depths greater than about 2600 m, liquid CO_2 is denser (*12*) than seawater (Fig. 4). We placed a frame containing a 4-liter beaker and a glass tube (diameter, 30 × 17.5 cm) on the ocean floor at a depth of 3627 m and a temperature of 1.6°C. In this region the liquid CO_2 should be significantly denser than the local seawater and less dense than the hydrate. Liquid CO_2 in the beaker was exposed only to seawater, whereas the CO_2 in the open tube was exposed to seawa-

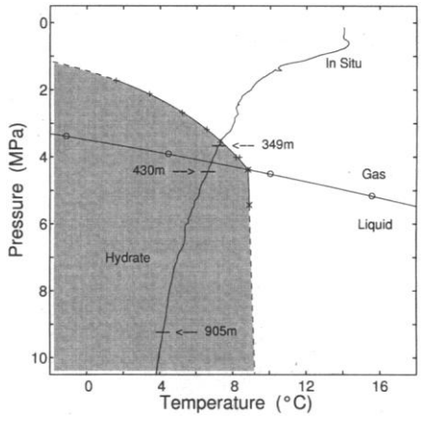

Fig. 1. A typical ocean water column temperature-pressure profile (solid line) for the experimental area off Monterey Bay, California, with the phase boundaries for the gas-liquid transition of CO_2 (○) and CO_2 hydrate formation (+, the gas-seawater hydrate boundary; ×, liquid CO_2-seawater hydrate boundary) overlaid for reference. The quadruple point, where all four phases coexist, is indicated (*). Shaded region is the area where CO_2 hydrate is stable if a sufficient amount of CO_2 is present. Depths for four of the five releases are indicated: experiment 1 at 349 m, experiment 2 at 430 m, and experiments 3 and 4 at 905 m. At this latitude and in this depth interval, 1 MPa is approximately equivalent to 99 m.

[1]Monterey Bay Aquarium Research Institute, Post Office Box 628, Moss Landing, CA 95039, USA. [2]School of Earth Sciences, Stanford University, Stanford, CA 94305, USA.

*To whom correspondence should be addressed. E-mail: brpe@mbari.org

ter on the upper surface and to sediment on the lower surface. The surrounding sediment was also used for free-release studies.

The beaker was filled (*10*) about half full with CO_2, which was expelled slowly from a small-bore tube. Initially, the individual drops did not coalesce; instead they appeared as of a pile of translucent marble-sized spheres. When they did coalesce, the surface of the CO_2 phase had a strongly curved and lobate shape. A significant increase in volume was soon observed. About 100 min after the initial release, the CO_2 phase volume had increased to fill the beaker. As the volume continued to increase, the liquid CO_2 overflowed onto the sea floor (Fig. 5). Fifteen similar overflow events occurred over the next 80 min (*13*). Some hydrate was formed at the bottom of the beaker early in the experiment. Its translucence and optical properties, closely similar to the liquid phase, made it difficult to determine the amount and exact position of the solid-liquid interface.

About 1.8 liters of liquid CO_2 was also delivered into the larger tube (volume, about 7 liters) and exposed to the sea floor at one end. Again, the individual drops eventually coalesced into a larger mass and the volume increased steadily to cause overflow after 283 min. Motions at the surface were easily observed, with schlieren in the overlying seawater, presumably from the dissolution of CO_2, the release of heat, and the rejection of salt by the hydrate-formation process.

The CO_2 that spilled onto the sea floor did not penetrate or appear to react with the sediment in any way. It was highly mobile and, because the experimental site was on a slight slope, much of the material rolled out of view. Sediment particles did not stick to its surface as it moved. We excavated a small hole in the sediment in an attempt to contain the material. However, the density of the CO_2 globules was only slightly greater than that of the surrounding seawater and passing eddies easily disturbed the liquid. The strong surface tension of the CO_2 resulted in disappearance of the entire blob as a unit. Freely released CO_2 was so mobile that it was difficult to determine whether volume changes were occurring. In addition, the presumed presence of a hydrate skin did not impede movement of the CO_2 globules on the sea floor (*14*).

Reaction of 1 mol of CO_2 with 5.75 mol of water to produce hydrate should yield an increase in volume of about a factor of 3 under these conditions; we observed a volume increase much larger than this, perhaps as much as a factor of 4 to 7. Thus, it appears that a metastable phase with a large number of vacancies and trapped brine formed in the first few hours, displacing the remaining liquid CO_2 upward and forcing overflow. Attempts to model this process have been published (*15, 16*). Had our experiment been sited much deeper, a floating skin of hydrate probably would have formed over the denser liquid CO_2. We calculate that this would occur at a depth of more than 4500 m. We were not able to observe the complete cycle of massive hydrate formation and dissolution. A thruster failure after 13 hours forced us to terminate the experiment. When we lifted the experimental frame, a block of ~7 liters of hydrate, formed in the open-ended tube, slid out and stood as a column on the sea floor. The near equivalence of the index of refraction of hydrate and seawater made visualization difficult.

These experiments imply that liquid CO_2 on the sea floor, in the depth range 2700 to 4500 m, would quickly react with water, form hydrate, and swell to many times its original size. A rough approximation of rates based on these observations (*17*) suggests that the rate of hydrate formation was about 1.2 liters/hour. If we assume formation of a $CO_2 \cdot 6H_2O$ hydrate, then the rate of water incorporation is about 0.94 liter/hour. This reaction is strongly exothermic [271 kJ/(kg of water)] (*18*); thus, the upper interface is releasing considerable heat and rejected brine.

Ideas of "permanent" disposal of CO_2 as a hydrate on the sea floor probably are not realistic, although quite long residence times may very well be possible—first in the hydrate phase and later because of the long ocean circulation time scales. The necessity for equality of chemical potential in all three phases as a condition for hydrate stability [$\mu_{aq} = \mu_{CO2} = \mu_{clath}$] has long been known (*19*), but background ocean CO_2 levels are far from saturation. Ocean disposal of CO_2 remains attractive for the basic reasons of enormous reservoir size, the ability of the carbonate sediments to restore buffer capacity, the long circulation times of the ocean, and a

Fig. 2. Image of CO_2 hydrate formation from the gas phase at a 349-m depth, T = 8°C, showing white hydrate rind on the bubble skin. Image overlay shows depth in meters (top left) and date time (bottom right).

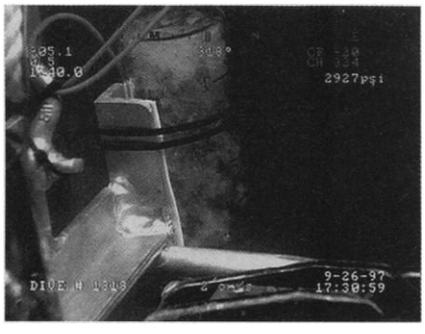

Fig. 3. Mass of flocculant CO_2 hydrate created at a 905-m depth, T= 4°C, by vigorous injection of liquid CO_2 through a small-bore tube. The pure hydrate density is greater than that of seawater but at the time of formation in this manner occluded liquid CO_2 and trapped water warmed by the heat of formation create a buoyant mass.

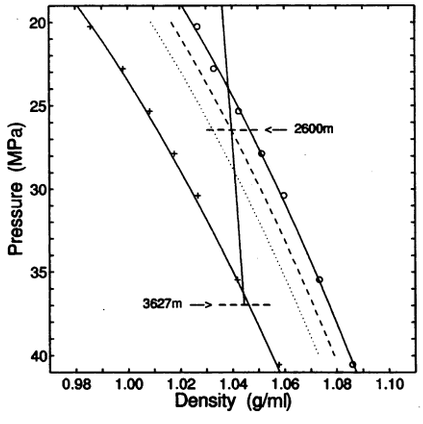

Fig. 4. Pressure-density curves of liquid CO_2 at various temperatures overlaid on the pressure-density profile for our experimental region. The curves for 0°C (o) and 10°C (+) were fit to experimental data; the curves for 4°C (···) and 2°C (---) were obtained by linear interpolation. In practice the neutrally buoyant point is reached at about 26.50 MPa (2600 m). Our controlled release took place at 36.95 MPa (3627 m) and the ambient temperature was 1.6°C.

Fig. 5. Overflow of liquid CO_2 from the 4-liter beaker onto the sea floor at a 3650-m depth. A mass of transparent hydrate ($CO_2 \cdot 5.75H_2O$), formed at the upper interface, sank to the bottom of the beaker and pushed out the remaining liquid CO_2. Ejected liquid CO_2 was highly mobile and did not appear to penetrate, or interact with, the sediments.

favorable equilibrium with the atmospheric reservoir. Formation of a hydrate is but one component of the ocean disposal process, and it can have a dramatic effect.

References and Notes

1. W. S. Broecker, *Science* **278**, 1582 (1997); C. Hanisch, *Environ. Sci. Technol.* **32**, 20A (1998); E. A. Parson and D. W. Keith, *Science* **282**, 1053 (1998).
2. J. T. Houghton *et al.*, *Climate Change: The IPCC Scientific Assessment* (Intergovernmental Panel on Climate Change, Cambridge Univ. Press, Cambridge, UK, 1990).
3. P. G. Brewer, *Geophys. Res. Lett.* **24**, 1367 (1997); C. Goyet *et al.*, *J. Mar. Res.* **57**, 135 (1999).
4. For injections at depths of <1000 m we used the R/V *Point Lobos* and ROV *Ventana*. The 3627-m experiment was carried out using the R/V *Western Flyer* and the ROV *Tiburon*. The R/V *Western Flyer* is a 35.7-m SWATH (small waterplane area twin hull) ship with a center "moon pool" for ROV deployment. *Tiburon* is a 4000-m capable ROV attached to the mother ship by an armored steel cable with both copper power conductors and single-mode optical fibers for communication and control. Six 3.7-kW electric thrusters supply thrust. The vertical ascent speed is 100 feet/min (30.48 m/min). The experiments were imaged by the vehicle cameras and data were recorded on videotape. The *Ventana* observations were made with a Sony DXC-3000 three-chip camera, and the *Tiburon* made observations with two Panasonic VW E5550 three-chip cameras, with data recorded in digital beta format. Ocean temperature, pressure, and conductivity were sensed continually by a CTD package (Falmouth Scientific) attached to either vehicle within 2 m of the experimental chambers.
5. P. G. Brewer, F. M. Orr Jr., G. Friederich, K. A Kvenvolden, D. L. Orange, *Energy Fuels* **12**, 183 (1998).
6. G. D. Holder, A. V. Cugini, R. P. Warzinski, *Environ. Sci. Technol.* **28**, 276 (1975); I. Aya, K. Yamane, H. Nariai, *Energy* **22**, 263 (1997).
7. K. H. Cole, G. R. Stegen, D. Spencer, *Energy Convers. Manage.* **34**, 991 (1993); D. Archer, H. Kheshgi, E. Maier-Reimer, *Geophys. Res. Lett.* **24**, 405 (1997).
8. E. D. Sloan Jr., *Clathrate Hydrates of Natural Gases* (Dekker, New York, 1990).
9. W. J. North, V. R. Blackwell, J. J. Morgan, *Environ. Sci. Technol.* **32**, 676 (1998).
10. Liquid CO_2 injections were carried out by expulsion from a reservoir by a piston, activated on command from the vehicle control room. For the shallow releases a small volume (~500 ml) steel cylinder was used. For the 3627-m experiment about 9 liters of liquid CO_2 was contained in a commercial accumulator (Parker A4N0578D1) installed horizontally in the tool sled frame. The accumulator was connected to a set of valves and fittings, which permitted loading of the cylinder with liquid CO_2 from standard gas cylinders before the dive. Procedurally, after the first filling, an accumulator gauge pressure of about 600 pounds per square inch (psi) was observed, with the piston set at maximum accumulator capacity. The gas delivery cylinder was then warmed (to compensate for expansion cooling on CO_2 transfer), and the accumulator was packed in ice to lower the temperature of the contained CO_2. A second filling was carried out, and the ice was removed. The filled accumulator was vented to about 750 psi as it warmed to room temperature to prevent overpressure. The system was configured to permit open contact between seawater and the ocean side of the accumulator piston. As the vehicle dived, and pressure increased, the decrease in volume of the contained liquid CO_2 was compensated for by active piston motion to maintain pressure equality. Camera inspection of the pressure gauge during the dive showed the expected drop in accumulator pressure as the pressure-temperature boundary for liquid CO_2 was approached (in practice at a depth of about 400 m), and the differential pressure across the piston dropped effectively to zero. A system check was carried out by opening the quarter-turn CO_2 release valve at several depths during deployment, thereby venting small amounts of liquid CO_2.
11. *Third International Conference on Carbon Dioxide Removal* [Cambridge, MA, Sept. 1996, supplement to *Energy Conversion and Management* **38** (1997)]; R. Socolow, Ed., *Fuels Decarbonization and Carbon Sequestration* (Princeton University CEES Report No. 302, 1997) (www.princeton.edu/~ceesdoe).
12. W. J. Harrison, R. F. Wendtland, E. D. Sloan Jr., *Appl. Geochem.* **10**, 461 (1995).
13. Images of the overflow events are posted along with other supplementary material at www.sciencemag.org/feature/data/987369.shl and at the Monterey Bay Aquarium Research Institute (MBARI) Web site www.mbari.org/ghgases/deep/release.htm
14. H. Sakai *et al.*, *Science* **248**, 1093 (1990).
15. R. Ohmura and Y. H. Mori, *Environ. Sci. Technol.* **32**, 1120 (1998).
16. Y. Fujioka, K. Takeuchi, M. Ozaki, Y. Shindo, H. Komiyama, *Int. J. Energy Res.* **19**, 659 (1995).
17. The total volume of the glass tube was ~7.22 liters (diameter, 30 × 17.5 cm) and the initial volume of liquid CO_2 was 1.8 liters. It is possible to calculate the minimum rate of water incorporation, assuming that the rate of filling [(7.2 liters − 1.8 liters)/4.5 hours = 1.2 liters/hour] was equivalent to hydrate formation, hydrate density was 1.1 kg/liter, and water accounted for 71% of the mass of the hydrate ($CO_2 \cdot 6H_2O$): rate = 1.2 liters/hour × 1.1 kg/liter × 0.71 = 0.94 kg/hour. The actual rate is somewhat faster as some CO_2 is incorporated into the hydrate.
18. K. Ohgaki, Y. Makihara, K. Takano, *J. Chem. Eng. Jpn.* **26**, 558 (1993).
19. R. J. Bakker, J. Dubessy, M. Cathelineau, *Geochim. Cosmochim. Acta* **60**, 1657 (1996).

20. Supported by a grant to MBARI from the David and Lucile Packard Foundation. We thank the MBARI engineers, ROV pilots, and ships' crews for their skilled support.

29 December 1998; accepted 6 April 1999

Spectroscopic Determination of the Water Pair Potential

R. S. Fellers,[1] C. Leforestier,[2] L. B. Braly,[1] M. G. Brown,[1] R. J. Saykally[1]*

A polarizable water pair potential was determined by fitting a potential form to microwave, terahertz, and mid-infrared $(D_2O)_2$ spectra through a rigorous calculation of the water dimer eigenstates. It accurately reproduces most ground state vibration-rotation-tunneling spectra and yields excellent second viral coefficients. The calculated dimer structure and dipole moment are very close to those determined from microwave spectroscopy and high-level ab initio calculations. The dimer binding energy and acceptor switching and donor-acceptor interchange tunneling barriers are in excellent agreement with recent ab initio theory, as are cyclic water trimer and tetramer structures and binding energies.

Much experimental and theoretical effort has been directed toward understanding the nature of the water dimer: the archetype for aqueous hydrogen bonding. Although the dimer structure and hydrogen bond rearrangement dynamics are now fairly well characterized, the equilibrium binding energy (D_e) and dissociation energy (D_0) remain controversial, and these are crucial for properly assessing recently proposed dimer effects in atmospheric chemistry (*1*). Water dimer properties are most succinctly and profoundly expressed in the intermolecular potential energy surface (IPS)—the water pair potential. This pair potential is likewise essential for modeling the condensed phases of water, because it is the principal component of the force field (three- and four-body interactions are much weaker). The water pair potential has heretofore eluded accurate determination because of technological and computational impediments. Here we describe the determination of a polarizable water pair potential by regression analysis of the rotational constants, tunneling splittings, and intermolecular vibrational frequencies precisely determined from microwave, terahertz, and infrared vibration-rotation-tunneling (VRT) spectroscopy of the water dimer (*2*, *3*). Our previous experience with simpler IPS determinations indicates that such measurements provide an exacting measure of the relevant force field (*4*).

Theoretical and spectroscopic studies have shown that the six-dimensional (6D) water IPS has a complex topology. There are eight identical global minima, differing only by permutations of the four hydrogen atoms and two oxygens that do not break covalent bonds [the permutation-inversion symmetry group is $D_{4h}(M)$]. Ab initio calculations (*5*) have revealed three low-energy paths connecting these eight degenerate minima: "acceptor switching" (equivalent to a 180° rotation of the hydrogen bond acceptor about its symmetry axis), "interchange" (exchange of the role of donor and acceptor of the hydrogen bond), and "bifurcation" (exchange of bound and free hydrogens

[1]Department of Chemistry, University of California, Berkeley, CA 94720–1460, USA. [2]Laboratoire Structure et Dynamique des Systèmes Moléculaires et Solides (UMR 5636), CC 014, Université des Sciences et Techniques du Langue-doc, 34095 Montpellier Cédex 05, France.

*To whom correspondence should be addressed. E-mail: saykally@uclink4.berkeley.edu